

Photo-Cured Organic–Inorganic Hybrid Composites of Acrylated Castor Oil and Methacrylate-Substituted Polysilsesquioxane

Mitsuhiro Shibata, Syotarou Obara

Department of Life and Environmental Sciences, Faculty of Engineering, Chiba Institute of Technology, 2-17-1 Tsudanuma, Narashino, Chiba 275-0016, Japan

Received 14 August 2011; accepted 28 November 2011

DOI 10.1002/app.36582

Published online in Wiley Online Library (wileyonlinelibrary.com).

ABSTRACT: Acrylated castor oil (ACO) was synthesized by the reaction of castor oil and acryloyl chloride in the presence of triethylamine. The $^1\text{H-NMR}$ and Fourier transform infrared spectral analyses of ACO showed that the hydroxy groups of castor oil are completely esterified and that the number of acrylate groups per triglyceride is 2.56. The ACO was photo-cured with methacrylate-substituted polysilsesquioxane (ME-PSQ) prepared from 3-(trimethoxysilyl)propyl methacrylate and tetramethylammonium hydroxide in the ACO/ME-PSQ weight ratio of 20/0, 20/1, 20/2, and 20/3. Although the mechanical reinforcement effect by the incorporation of PSQ frameworks was observed when eval-

uated from dynamic mechanical analysis and flexural test, the reinforcement effect showed a tendency to decline with a higher ME-PSQ content. The TEM observation revealed that the PSQ is homogeneously distributed in the matrix for the cured ACO/ME-PSQ (20/1), while some aggregated particles of the PSQ were observed for the cured AC/ME-PSQ (20/2). The 5% weight loss temperature of the cured ACO/ME-PSQ rose with ME-PSQ content. © 2012 Wiley Periodicals, Inc. *J Appl Polym Sci* 000: 000–000, 2012

Key words: nanocomposites; renewable resources; photopolymerization; acrylated castor oil; silsesquioxane

INTRODUCTION

The use of renewable resources as replacement materials for industrial products is attracting great interest with increasing emphasis on environmental issues, waste disposal, and depletion of earth's limited petroleum reserves.^{1,2} Among the renewable natural resources, triglyceride plant oils represent a major class of such resources and are being used in an increasing number of industrial applications, in addition to being a food sources.^{3,4} Castor oil is a relatively inexpensive plant oil obtained from the seed of *Ricinus communis*.⁵ It is a triglyceride in which approximately 90% of the fatty acid chains are ricinoleic acid, that is, (9Z, 12R)-12-hydroxyoctadec-9-enoic acid, as is shown in Figure 1. Because of its hydroxy functionality, the oil is suitable for use in isocyanate reactions to synthesize cost-effective polyurethane elastomers.^{6–10} In this study, acrylated castor oil (ACO) was synthesized by the reaction of castor oil and acryloyl chloride in the presence of triethylamine. To use the ACO as a photo-cured coating material in a manner similar to conventional petroleum-based acrylate resins, the improvement of

the thermal and mechanical properties is necessary because ACO has three aliphatic long chains in the molecule.

Organic–inorganic hybrid composites by the reaction of polysilsesquioxanes ($\text{RSiO}_{3/2}$)_n with organic functional groups with organic monomers, oligomers, and polymers possessing functional groups are expected to have increased performance capabilities relative to the former non-hybrid nanocomposites.^{11–16} We had already reported that organic–inorganic hybrid composites of itaconate unit-incorporated poly(butylene succinate)¹⁷ and terpene acrylate resins¹⁸ with methacrylate-substituted polysilsesquioxanes (ME-PSQ) prepared from 3-(trimethoxysilyl)propyl methacrylate (TMSPM) have greater thermal and mechanical properties than the cured control materials without ME-PSQ. The present study describes the synthesis of ACO and the thermal and mechanical properties of the photo-cured mixture of ACO and ME-PSQ (C-ACO/ME-PSQ).

EXPERIMENTAL

Materials

Castor oil (iodine value: 86 g-I₂/100g; hydroxy value: 152.3 mg-KOH/g) was kindly supplied from Itoh Oil Chemicals Co., Ltd. (Yokkaichi, Mie, Japan). Acryloyl chloride, acrylic acid, and triethylamine

Correspondence to: M. Shibata (shibata@sky.it-chiba.ac.jp).

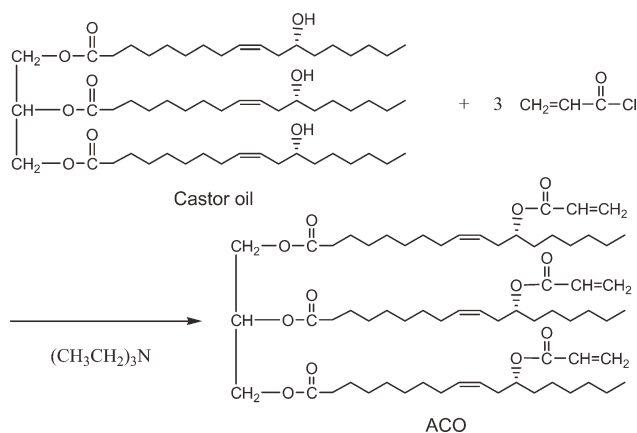


Figure 1 Synthetic scheme of ACO.

were purchased from Tokyo Chemical Industry Co., Ltd. (Tokyo, Japan). Photo-initiators, 1-hydroxycyclohexyl phenyl ketone (Irgacure 184, m.p. 45–49°C, UV/VIS absorption peaks in methanol: 246, 280, 333 nm) and phenyl bis(2,4,6-trimethylbenzoyl)phosphine oxide (Irgacure 819, m.p. 127–133°C UV/VIS absorption peaks in methanol: 295, 370 nm) were kindly supplied from Chiba Specialty Chemicals K.K. (Tokyo, Japan). TMSPM and 10 wt % tetramethylammonium hydroxide (TMAOH) in water were purchased from Sigma-Aldrich Japan Co., Ltd. (Tokyo, Japan).

Preparation of ACO

Synthetic scheme of ACO is shown in Figure 1. To a solution of castor oil (80.1 g, OH 0.217 mol) and triethylamine (25.8 g, 0.255 mol) in benzene (250 mL) was added acryloyl chloride (23.1 g, 0.255 mol) dropwise at 5–10°C. After stirring for 24 h at room temperature, the reaction mixture was filtered and the filtrate was washed with 5% aqueous sodium bicarbonate, and then washed with ion-exchanged water. The benzene solution was dried over sodium sulfate, and evaporated to produce ACO as colorless viscous liquid (74.4 g) with a 81% yield: $^1\text{H-NMR}$ in CDCl_3 , δ (ppm) 6.38(d, acryl H-A), 6.10(d, acryl H-

B), 5.80 (d, acryl H-C), 5.47 (m, H-9), 5.35 (m, H-10), 5.30 (m, H-2'), 4.96 (m, H-12), 4.30 and 4.14 (m, H-1' and H-3'), 2.31 (m, H-2,11), 2.00 (m, H-8), 1.7–1.2 (m, H-3–7, H-13–17), 0.87 (m, H-18); Fourier transform infrared (FTIR) (cm^{-1}) 3020, 2931, 2858, 1747, 1724, 1470, 1412, 1385, 1300, 1273, 1196, 1049, 987, 984, 814.

Preparation of ME-PSQ

Synthetic scheme of ME-PSQ is shown in Figure 2. To a mixture of ion-exchanged water (25 mL), ethanol (75 mL), and 10 wt % TMAOH aqueous solution (1.0 mL, 1.1 mmol) were added TMSPM (20 mL, 84 mmol). The mixture was stirred for 24 h at room temperature, and allowed to stand for 1 day. The formed precipitate was collected by decantation, washed by vacuum filtration with ion-exchanged water/ethanol (1/3 by volume), and then washed again with ethanol. The rinsed product was dried under vacuum for 24 h at room temperature to give ME-PSQ (8.4 g) as a colorless viscous liquid with a 56 % yield: $^1\text{H-NMR}$ in CDCl_3 δ (ppm) 6.04 (bs, olefinic H-f), 5.52 (bs, olefinic H-e), 4.05 (bs, $\text{OCH}_2\text{CH}_2\text{CH}_2\text{Si}$), 1.90 (s, CH_3), 1.72 (bs, $\text{OCH}_2\text{CH}_2\text{CH}_2\text{Si}$); FTIR (cm^{-1}) 2959, 2951, 2912, 1713, 1639, 1454, 1408, 1319, 1296, 1115, 1018, 977, 814, 791, 763.

Preparation of C-ACO/ME-PSQ

In a ϕ 45 mm poly(tetrafluoroethylene) culture dish, ME-PSQ (0.25 g, methacryloyl group 1.39 mmol) and acetone (2.0 mL) were added and then irgacure 184 (50 mg, 0.24 mmol) and irgacure 819 (10 mg, 0.024 mmol) as surface and through cure initiators, respectively, were added. The mixture was heated to 70°C, and stirred for 1 h at 70°C. To the obtained mixture was added a solution of ACO (5.00 g, acryl 11.8 mmol) in acetone (2 mL). The mixture was heated to 120°C, stirred for 1 h at the temperature, and then allowed to stand at 60°C *in vacuo* for degassing. The obtained homogeneous mixture was photo-cured at room temperature for 10 min to produce a cured ACO/ME-PSQ (C-ACO/ME-PSQ) 20/1 composite

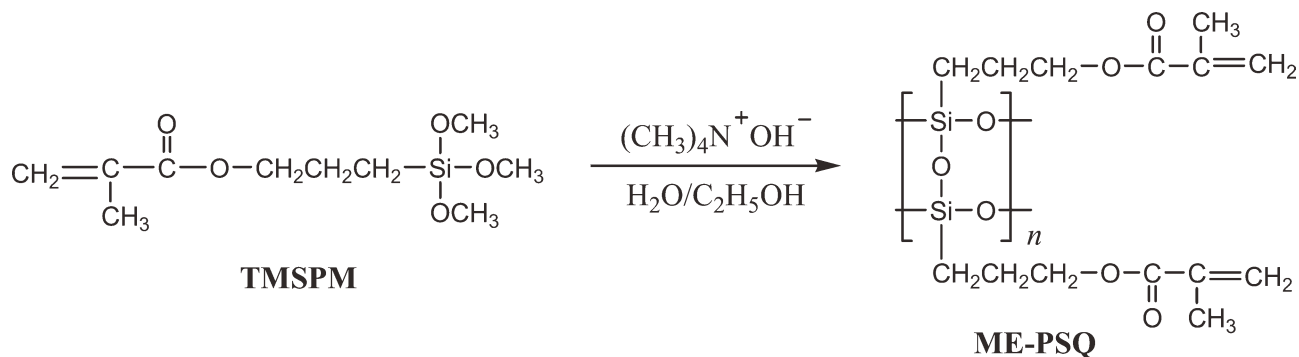


Figure 2 Synthetic scheme of ME-PSQ.

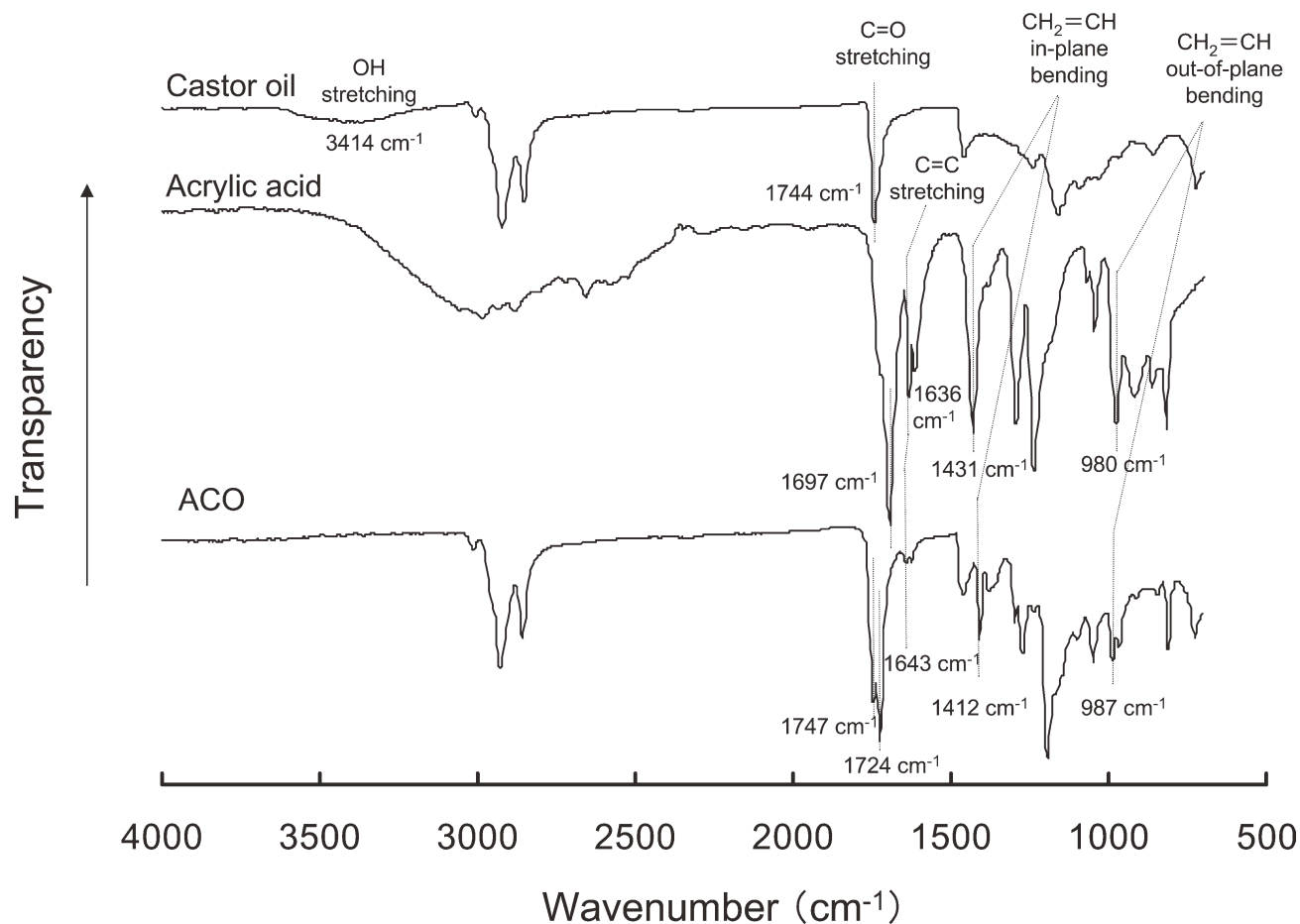


Figure 3 FTIR spectra of castor oil, acrylic acid, and ACO.

film (thickness: ca. 1.2 mm) with ME-PSQ content 5 parts per hundred parts by weight of resin (phr). SPOT-CURE SP-7 (250 W light source, wavelength 240–440 nm, Ushio Inc., Yokohama, Japan) was used for the photo-curing (irradiation intensity 60.6 mW/cm²). The C-ACO/ME-PSQ composites with the weight ratio 20/2 and 20/3 (ME-PSQ content: 10 and 15 phr) were prepared in a manner similar to the C-ACO/ME-PSQ 20/1 composite.

Measurements

FTIR spectra were recorded on a Shimadzu (Kyoto, Japan) FTIR 8100 by the KBr-pellet or attenuated total reflectance (ATR) method. Proton nuclear magnetic resonance (¹H-NMR) spectra were recorded on a Bruker AV-400 (400 MHz) (Madison, WI) using CDCl₃ as a solvent. Gel permeation chromatography (GPC) of ME-PSQ was carried out at 40°C on a Shimadzu LC-10A series apparatus equipped with two PLgel 5 μm Mixed-D GPC columns (Polymer Laboratories Ltd., Church Stretton, UK, the linear range of molecular weight: 200–400,000) and a refractive index detector. *N,N*-Dimethylformamide (DMF) was used as an eluent at a flow rate of 0.5 mL/min.

Polystyrene standards with a narrow distribution of molecular weight (M_w : 580–377,400) were used for molecular weight calibration. Transmission electron microscopy (TEM) was performed on a H-500 electron microscope (Hitachi High-Technologies Corporation, Tokyo, Japan) with a 100 kV accelerating voltage. The films were sectioned into roughly 120 nm thin sections at –70°C using an ultramicrotome with a diamond knife and then mounted on 200 mesh copper grids. Dynamic mechanical analysis (DMA) of the rectangular plates (length 30 mm, width 8 mm, thickness 1.2 mm) were performed on a Rheograph Solid (Toyo Seiki Co., Ltd, Tokyo, Japan) with a chuck distance of 20 mm, a frequency of 1 Hz, and a heating rate of 2 °C/min. The 5% weight loss temperature was measured on a Shimadzu TGA-50 thermogravimetric analyzer at a heating rate of 20 °C/min in a nitrogen atmosphere. Flexural test of the rectangular plates (length 30 mm, width 8 mm, thickness 1.2 mm) was performed at room temperature using an Autograph AGS-500C (Shimadzu Co. Ltd.) based on the standard method for testing the flexural properties of plastics (JIS K7171-2008, ISO 178-2001). Span length was 20 mm, and the testing speed was 10 mm/min. Five

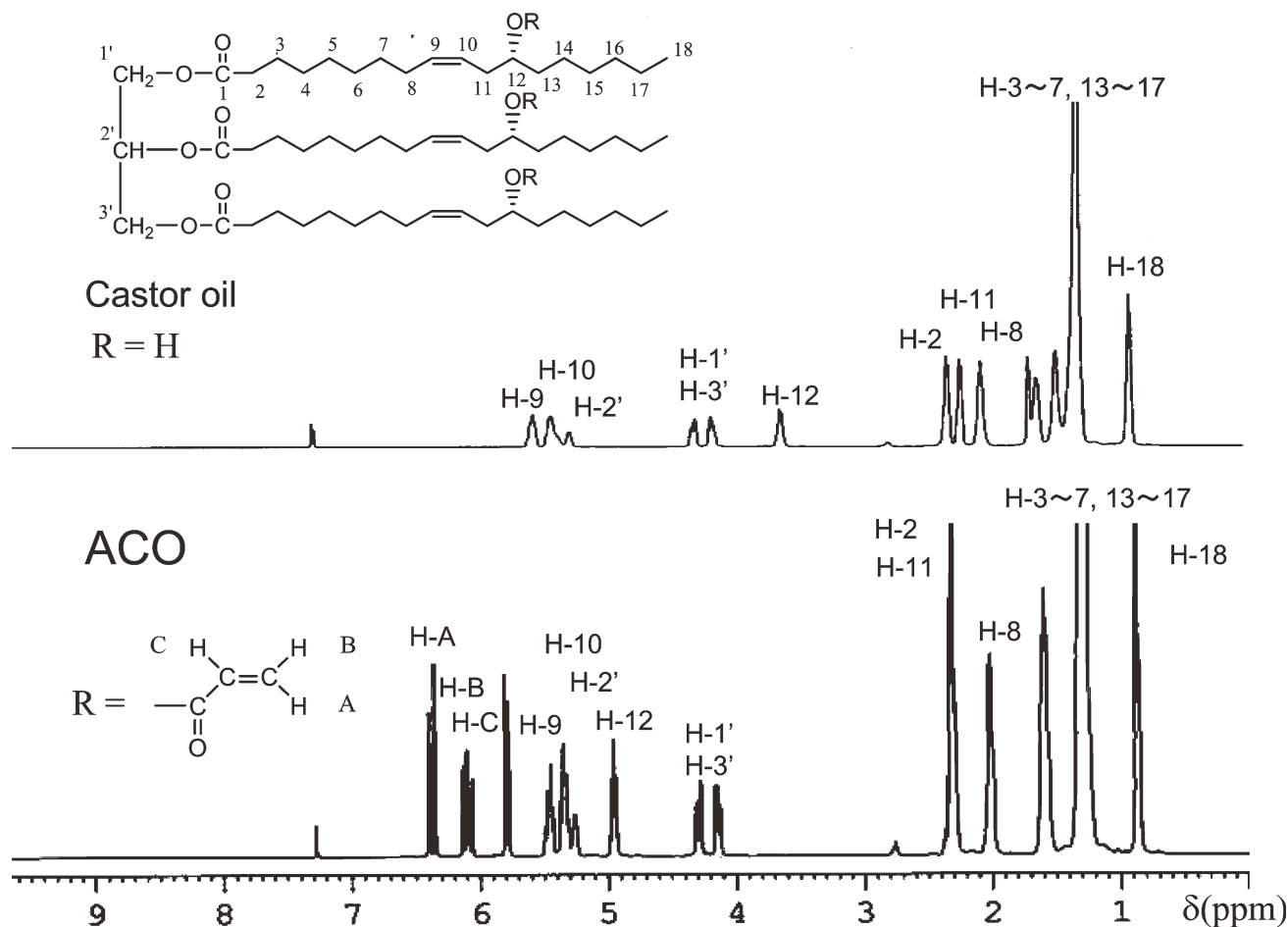


Figure 4 $^1\text{H-NMR}$ spectra of castor oil and ACO in CDCl_3 .

composite specimens were tested for each set of samples, and the mean values and the standard deviation were calculated.

RESULTS AND DISCUSSION

Characterization of ACO

Figure 3 shows the FTIR spectrum of ACO as compared with the spectra of castor oil and acrylic acid. The absorption peak at 1744 cm^{-1} for castor oil is ascribed to ester $\text{C}=\text{O}$ stretching vibration. In the case of ACO, the corresponding peak of triglyceride ester groups is observed at 1747 cm^{-1} , and the absorption peak at 1724 cm^{-1} is ascribed to acrylate ester $\text{C}=\text{O}$ stretching vibration. In the IR spectra of ACO and acrylic acid, the absorption peaks at 1643 and 1636 cm^{-1} are assigned to the stretching of vinyl attached to carbonyl group, the peaks at 1412 and 1431 cm^{-1} are corresponding to the olefinic C-H group in-plane bending, and the peaks at 987 and 980 cm^{-1} are corresponding to the olefinic C-H group out-of-plane bending, respectively. The absorption peak due to OH stretching vibration at

around 3414 cm^{-1} observed for castor oil disappeared for ACO, indicating that the esterification of castor oil with acryloyl chloride proceeded.

Figure 4 shows $^1\text{H-NMR}$ spectra of ACO and castor oil in CDCl_3 . ACO had the olefinic protons signals of acrylate group at 6.38 (H-A), 6.10 (H-B), and 5.80 ppm (H-C), which are not observed for castor oil. From the ratio of the acrylate protons to the terminal methyl protons (9H, H-18) of the triglyceride, the number of acrylate groups per a triglyceride molecule is evaluated to be 2.56. The number of hydroxyl groups per triglyceride for castor oil was calculated to be 2.53 from the hydroxyl value (152.3 mg-KOH/g) of castor oil and the molecular weight of triglyceride of ricinoleic acid (933.4). Therefore, it is estimated from the $^1\text{H-NMR}$ analysis that the hydroxyl groups of castor oil are completely esterified by the reaction with acryloyl chloride.

Characterization of ME-PSQ

Figure 5 shows $^1\text{H-NMR}$ spectrum of ME-PSQ. The ^1H -signals observed at 3.6 ppm of methoxy protons of TMSPM almost disappeared for ME-PSQ, and all

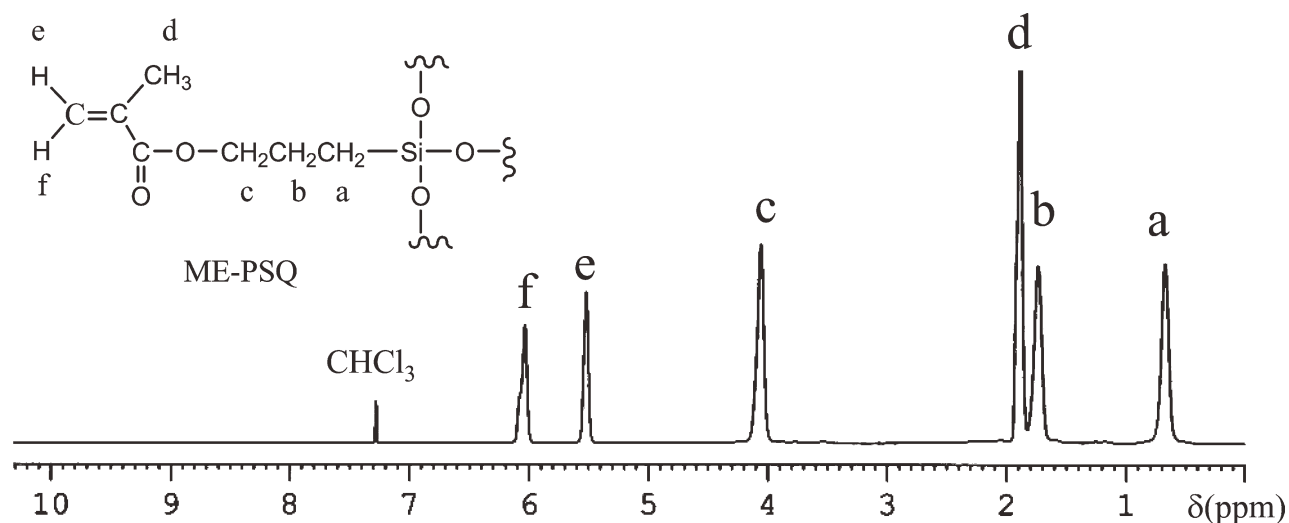


Figure 5 $^1\text{H-NMR}$ spectrum of ME-PSQ in CDCl_3 .

the protons of methacryloyloxypropyl group are observed, indicating the formation of silsesquioxanes. Figure 6 shows the FTIR spectra of ME-PSQ and TMSPM. TMSPM showed the absorption peaks due to methacryloyl $\text{C}=\text{O}$ and $\text{C}=\text{C}$ stretching vibrations at 1720 and 1639 cm^{-1} , respectively. The corresponding peaks characteristic of methacryloyl group were observed at 1713 and 1639 cm^{-1} for ME-PSQ. Although TMSPM showed the absorption peak due to $\text{Si}-\text{OCH}_3$ stretching vibration at 1083 cm^{-1} , ME-PSQ had the absorption peaks due to $\text{Si}-\text{O}-\text{Si}$ stretching vibration characteristics of $(\text{RSiO}_{2/3})_n$ moi-

ety at 1115 and 1018 cm^{-1} . It is known that the absorption peak due to $\text{Si}-\text{O}-\text{Si}$ stretching vibration for polyhedral oligomeric silsesquioxane (POSS), $(\text{RSiO}_{2/3})_8$, 10 , or 12 is observed at 1130 – 1115 cm^{-1} .¹⁹ Therefore, it is deduced that ME-PSQ is mainly composed of PSQs. We could not determine whether ME-PSQ contains POSS moiety or not from the FTIR spectral data.

The M_n and M_w measured by GPC using polystyrene standards for ME-PSQ were 5900 and $15,000$, respectively. The GPC chart is shown in Figure 7. The shoulder peak pointed by mark (a) is observed

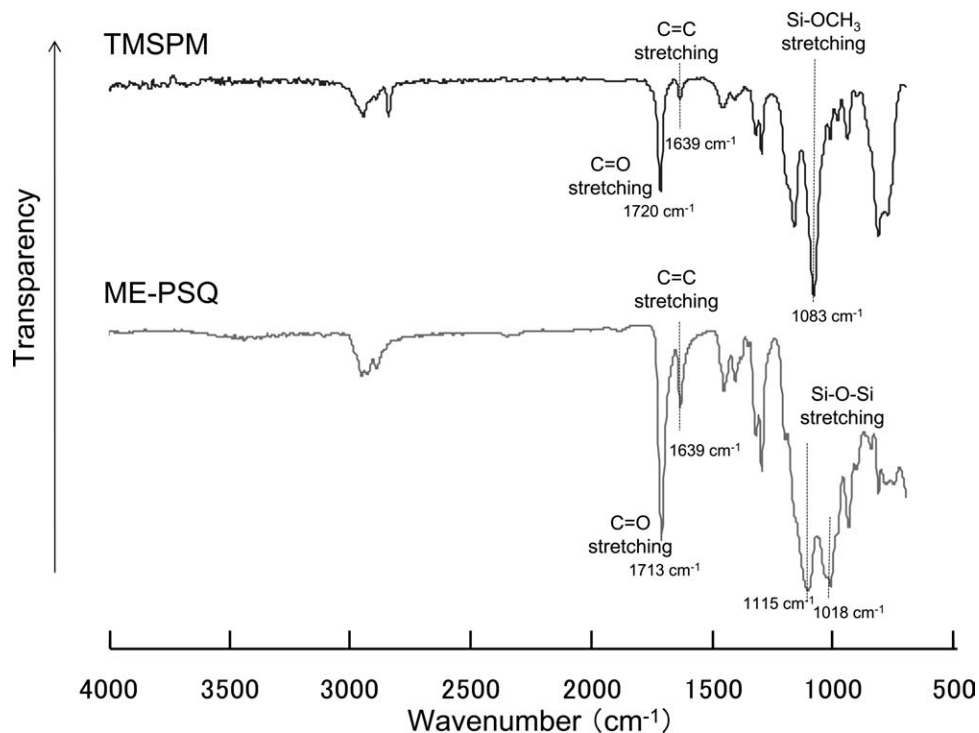


Figure 6 FTIR spectra of TMSPM and ME-PSQ.

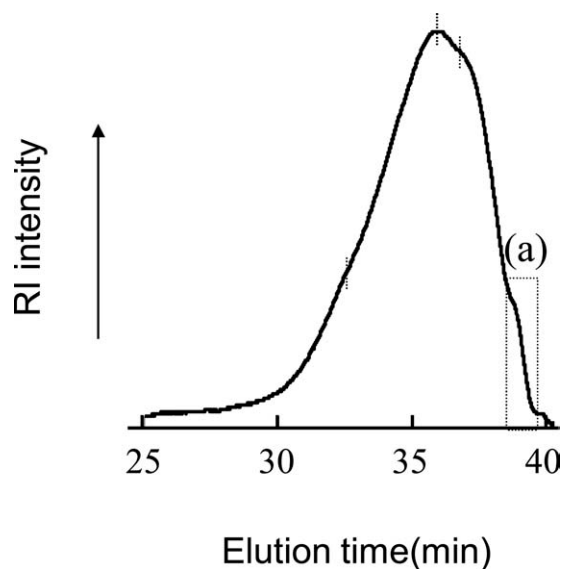


Figure 7 GPC chart of ME-PSQ.

at a lower molecular weight region. The M_n and M_w of the part (a) are 1600 and 1800, respectively. The M_n is close to the theoretical molecular weight (1432) of the corresponding cubic POSS, $(\text{RSiO}_{2/3})_8$. However, the GPC curve contained another two shoulder peaks at around 32.5 min and 36.7 min in addition to the main peak at 35.8 min and the shoulder peak of part (a). This result suggests that ME-PSQ contains PSQs with much higher molecular weight than the cubic POSS, such as ladder and ran-

dom PSQs shown in Figure 8 and/or bigger POSSs $(\text{RSiO}_{2/3})_{10,12}$, or 14 , etc.).

Characterization of C-ACO/ME-PSQ

Figure 9 shows the FTIR spectra of C-ACO/ME-PSQs as compared with CO, ACO, and photo-cured ACO (C-ACO). The absorption peaks at 1412 and 987 cm^{-1} due to olefinic C—H in-plane and out-of-plane bending observed for ACO were diminished for C-ACO, while their peaks still remained, indicating that photo-curing reaction of acryloyl groups is not completed. Although the sample was photo-irradiated longer than 10 min, the remaining peak was not diminished. On the other hand, the absorption peaks characteristic of acryloyl group disappeared for C-ACO/ME-PSQs with ME-PSQ contents 10 and 15 phr photo-irradiated for 10 min. The absorption peak at 725 cm^{-1} ascribed to CH=CH out-of-plane bending of ricinolate moiety observed for ACO little changed for the C-ACO/ME-PSQs, suggesting that most of the olefins at C-9 and C-10 positions are remaining after photo-curing.

Figure 10 shows TEM images of C-ACO/ME-PSQ composites with ME-PSQ contents of 5 and 10 phr. The fact that no phase separation was observed for C-ACO/ME-PSQ 5 phr indicates that the PSQ is homogeneously distributed in the matrix. On the other hand, some amount of aggregated particles with a diameter of about $0.1\text{--}2\text{ }\mu\text{m}$ appeared for C-

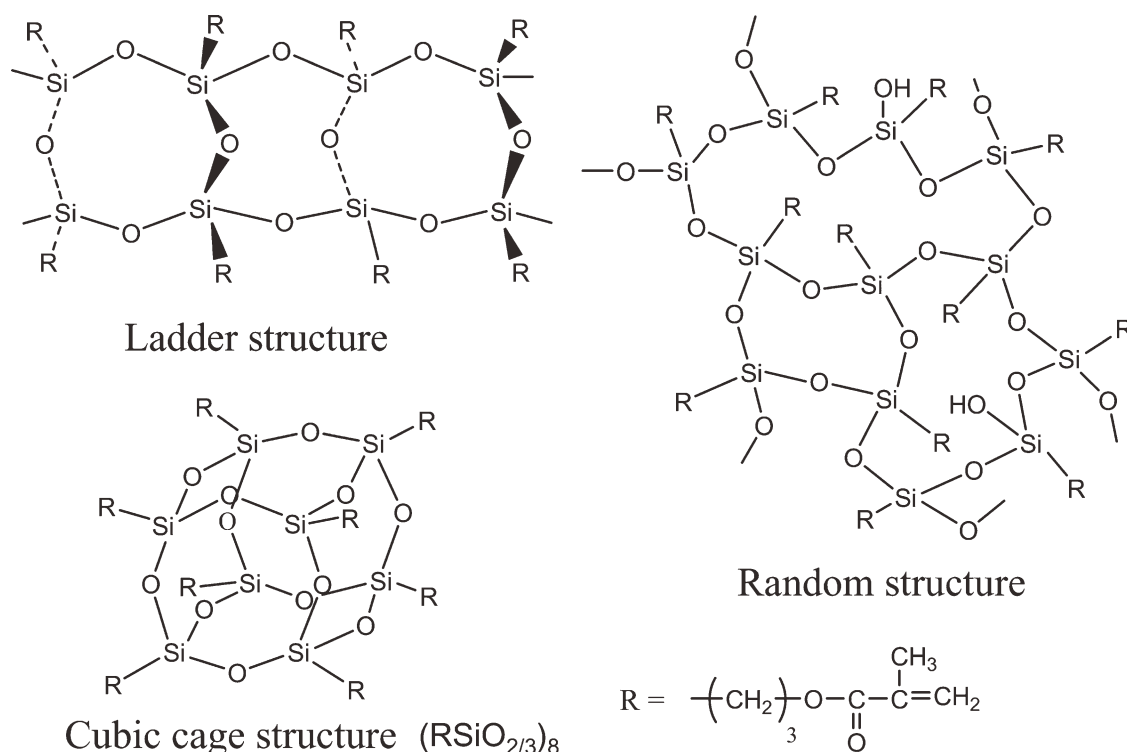


Figure 8 Probable structures of ME-PSQ.

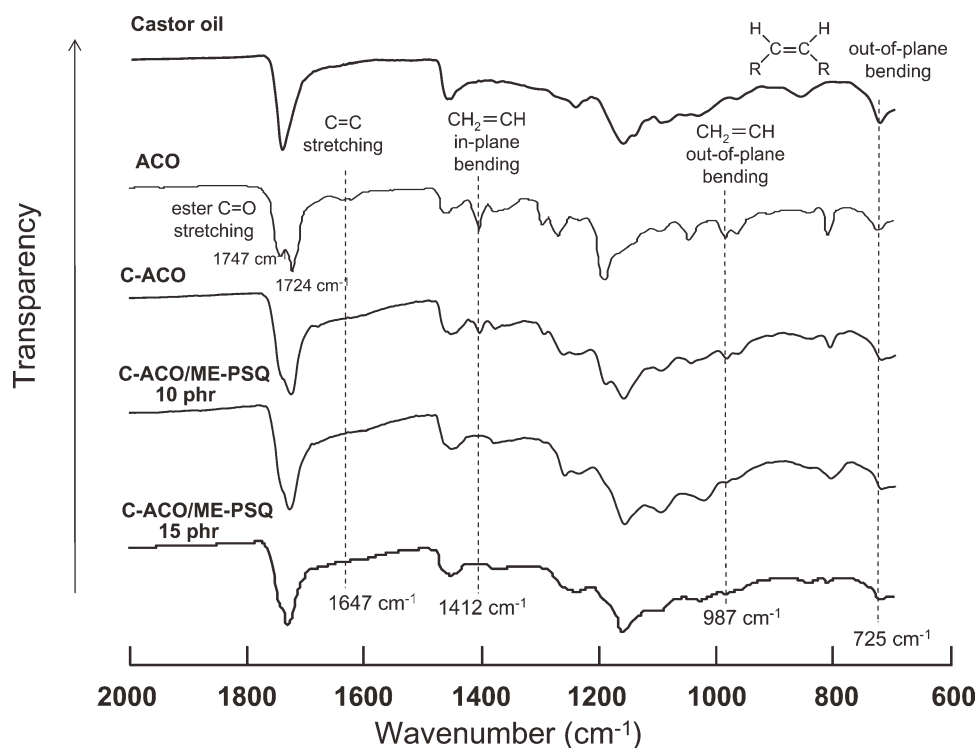


Figure 9 FTIR spectra of castor oil, ACO, C-ACO, and C-ACO/ME-PSQs.

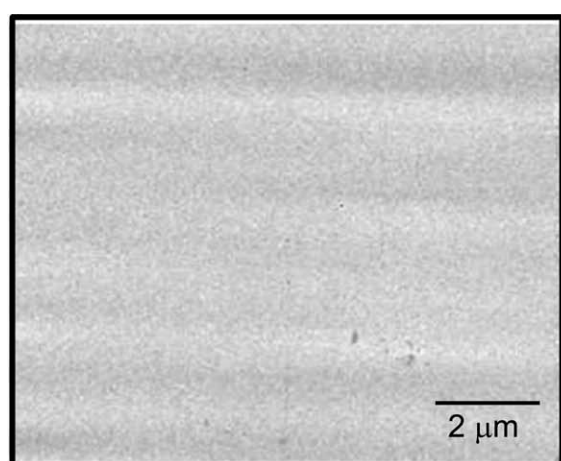
ACO/ME-PSQ 10 phr, indicating excess PSQ phase separated from the matrix.

Properties of C-ACO/ME-PSQ

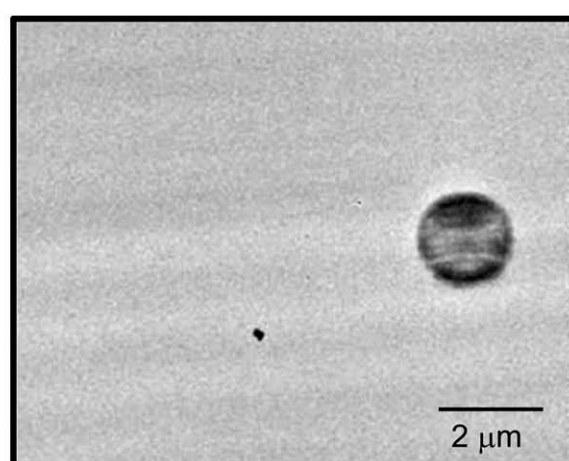
Figure 11 shows the temperature dependence of storage modulus (E') and $\tan \delta$ measured by DMA for C-ACO/ME-PSQ. The $\tan \delta$ peak temperature which is corresponding to glass transition temperature (T_g : -24.8 , -17.0 , -1.9 , -0.9°C) increased with increasing ME-PSQ content (0, 5, 10, and 15 phr).

The E' in a rubbery state over the temperature range from 20 to 120°C increased with increasing ME-PSQ content. As the difference in E' and T_g between C-ACO/ME-PSQ 10 phr and C-ACO/ME-PSQ 15 phr is less, the reinforcement effect showed a tendency to decline at ME-PSQ content 10–15 phr.

Figure 12 shows TGA curves of C-ACO/ME-PSQ. The 5% weight loss temperature of ME-PSQ (420.5°C) itself was much higher than that of C-ACO (349.7°C). The 5% weight loss temperature (357.6 , 363.0 , and 373.1°C) of C-ACO/ME-PSQ rose with ME-PSQ content (5, 10, and 15 phr).



C-ACO/ME-PSQ 5 phr



C-ACO/ME-PSQ 10 phr

Figure 10 TEM images of C-ACO/ME-PSQs (20/1 and 20/2).

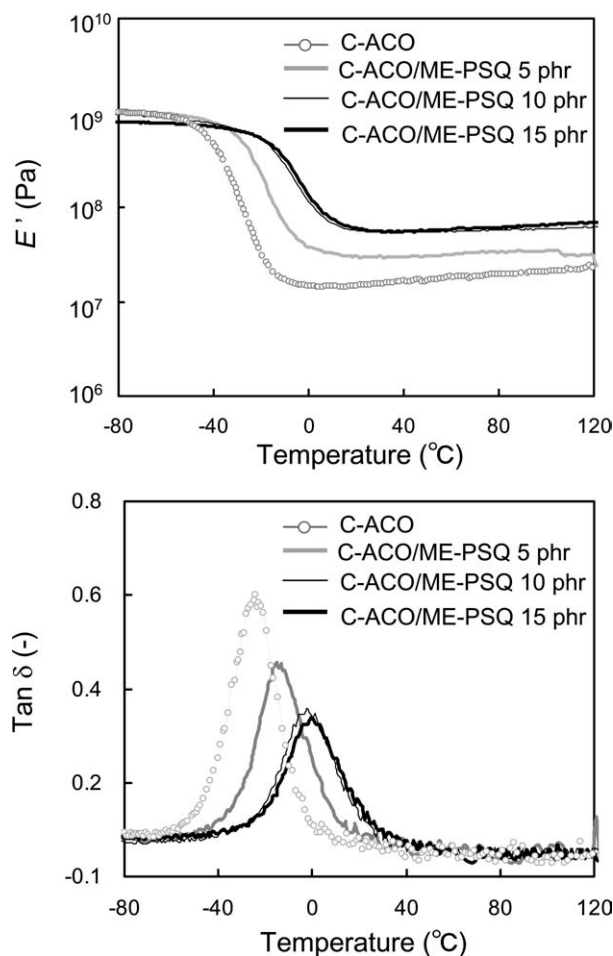


Figure 11 Temperature dependency of E' and $\tan \delta$ for C-ACO and C-ACO/ME-PSQs.

Figure 13 shows the flexural strength and modulus of C-ACO/ME-PSQ. The flexural strength and modulus for C-ACO/ME-PSQ also increased with an increase of ME-PSQ content. However, both the

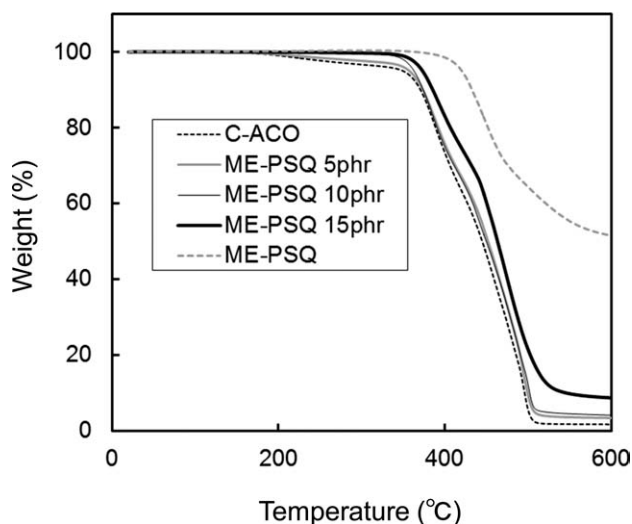


Figure 12 TGA curves of C-ACO, ME-PSQ, and C-ACO/ME-PSQs.

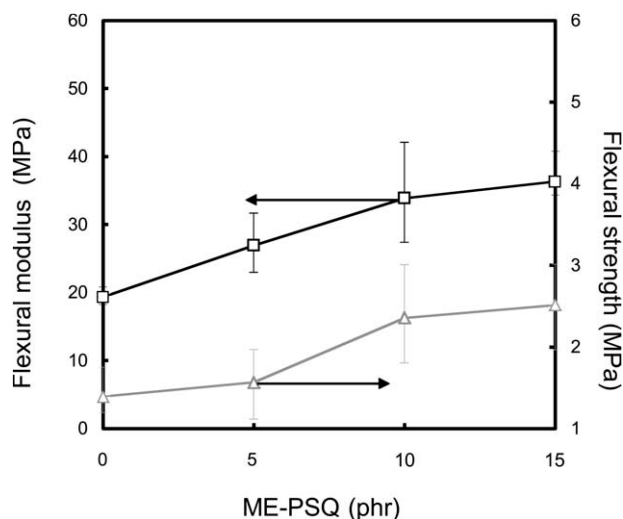


Figure 13 Flexural properties of C-ACO and C-ACO/ME-PSQs.

modulus and strength showed a tendency to level off at around ME-PSQ content 10–15 phr, in agreement with the result of DMA. The decline of the mechanical reinforcement effect should be related to the phase separation of the PSQ, as is obvious from Figure 10. The flexural strength and modulus of C-ACO/ME-PSQ 10 phr (2.36 and 33.9 MPa) showed 1.7–1.8 times higher than those of C-ACO (1.39, 19.3 MPa) in agreement with an increase of crosslinking density and the incorporation of rigid PSQ moiety.

CONCLUSIONS

The esterification of castor oil with acryloyl chloride produced ACO with the number of acrylate groups per triglyceride is 2.56. The hydrolysis and condensation reaction of TMSPM with TMAOH yielded ME-PSQ with M_n of 5900. The photo-curing of ACO and ACO/ME-PSQs (20/1, 20/2, and 20/3) produced C-ACO and C-ACO/ME-PSQs (20/1, 20/2 and 20/3) films, respectively. The TEM observation revealed that the PSQ is homogeneously distributed in the matrix for C-AC/ME-PSQ (20/1), while some aggregated particles of the PSQ were observed for C-AC/ME-PSQ (20/2). Storage modulus, $\tan \delta$ peak temperature, flexural strength, and modulus of C-ACO/ME-PSQ increased with increasing ME-PSQ content (0–10 phr). Their values showed a tendency to level off at ME-PSQ content 10–15 phr. The 5% weight loss temperature of C-ACO/ME-PSQ rose with ME-PSQ content.

References

1. Kaplan, D. L. In *Biopolymers from Renewable Resources*; Kaplan, D. L. Ed.; Springer-Verlag: Berlin Heidelberg, 1998; Chapter 1. p 1.

2. Mohanty, A. K.; Misra, M.; Hinrichsen, G. *Macromol Mater Eng* 2000, 276/277, 1.
3. Güner, F. S.; Yağı, Y. Y.; Erciyas, A. T. *Prog Polym Sci* 2006, 31, 633.
4. Sharma, V.; Kundu, P. P. *Prog Polym Sci* 2006, 31, 983.
5. Ogunniyi, D. S. *Bioresour Technol* 2006, 97, 1086.
6. Patel, P.; Suthar, B. *Polym Eng Sci* 1988, 28, 901.
7. Ogunniyi, D. S.; Fakayejo, W. R. O.; Ola, A. *Iranian Polym J* 1996, 5, 56.
8. Bai, S.; Khakhar, D. V.; Nadkarni, V. M. *Polymer* 1997, 38, 4319.
9. Jayabalan, M.; Lizymol, P. P. *Polym Degrad Stab* 1997, 58, 251.
10. Yeganeh, H.; Mehdizadeh, M. R. *Eur Polym J* 2004, 40, 1233.
11. Lichtenhan, J. D.; Vu, N. Q.; Carter, J. A.; Gilman, J. W.; Feher, F. J. *Macromolecules* 1993, 26, 2141.
12. Lichtenhan, J. D.; Otonari, Y. A.; Carr, M. J. *Macromolecules* 1995, 28, 8435.
13. Haddad, T. S.; Lichtenhan, J. D. *Inorg J Organomet Polym* 1995, 5, 237.
14. Yoon, K. H.; Park, J. H.; Min, B. G.; Polk, M. B.; Schiraldi, D. A. *Polym Int* 2005, 54, 47.
15. Hany, R.; Hartmann, R.; Böhlen, C.; Brandenberger, S.; Kawada, J.; Löwe, C.; Zinn, M.; Wilholt, B.; Marchessault, R. H. *Polymer* 2005, 46, 5025.
16. Liu, Y.; Yang, X.; Zhang, W.; Zheng, S. *Polymer* 2006, 47, 6814.
17. Sakuma, T.; Kumagai, A.; Teramoto, N.; Shibata, M. *J Appl Polym Sci* 2008, 107, 2159.
18. Ando, S.; Yoshihiro Someya, Y.; Tsutomu Takahashi, T.; Shibata, M. *J Appl Polym Sci* 2010, 115, 3326.
19. Arkles, B. *Silicon Compounds Register and Review*; Petrarch Systems: Bristol, PA, 1987.